Predictive Uncertainty in State-Estimation Drives Active Sensing in Weakly Electric Fish

Osman Kaan Karagoz[1,2], Aysegul Kilic[1], Emin Yusuf Aydin[3], Mustafa Mert Ankarali[1,2] and Ismail Uyanik[3,4*]

[1]Electrical and Electronics Engineering, Middle East Technical University, 06800, Ankara, Turkiye.
[2]Center for Robotics and AI, Middle East Technical University, 06800, Ankara, Turkiye.
[3]Bioengineering Division, Hacettepe University, 06800, Ankara, Turkiye.
[3*]Electrical and Electronics Engineering, Hacettepe University, 06800, Ankara, Turkiye.

*Corresponding author(s). E-mail(s): uyanik@ee.hacettepe.edu.tr; Contributing authors: okaragoz@metu.edu.tr; kilica@metu.edu.tr; eminyusufaydin@gmail.com; mertan@metu.edu.tr;

Abstract

Animals adapt their sensory systems to accurately perceive their environment and therefore achieve optimal behavioral performance under varying sensory conditions. In addition to sensory adaptation, we propose that animals employ active sensing movements to shape the spatial and temporal characteristics of sensory signals. However, the mechanisms governing the generation of active sensing movements within the neural circuits of the central nervous system are not known. To address this, we investigated the role of active sensing movements in the refuge tracking behavior of *Eigenmannia virescens*, a species of weakly electric fish. These fish track the longitudinal movements of a refuge in which they are hiding by swimming back and forth in a single linear dimension. During refuge tracking, *Eigenmannia* exhibits stereotyped whole-body oscillations, in addition to its tracking movements, when the quality of the sensory signals degrades. We developed a state-feedback sensorimotor control model of the fish to examine the role of these ancillary movements on the refuge tracking performance of the fish. Here we showed that

active sensing movements are tuned to minimize the predictive uncertainty in state estimation, working as a closed-loop controller in parallel with the behavioral task controller. We experimented with $\boldsymbol{N} = \mathbf{3}$ fish to demonstrate the predictive performance of the proposed model, specifically in terms of capturing the characteristics of the smooth-pursuit tracking and active sensing movements of the fish. Our systematic and comparative analysis suggests that the proposed predictive uncertainty-based active sensing generator model produces fish movements that have statistically indistinguishable trajectories from that of the actual fish movements, unlike the recent models present in the literature.

Keywords: active sensing, weakly electric fish, sensorimotor control, state estimation

1 Introduction

Active sensing is a dynamic process in which animals orchestrate feedback loops to refine their sensory inputs [1, 2]. It encompasses a range of intricate movements such as repositioning antennae in arthropods [3], eye rotations and saccadic movements in primates [4], and exploratory whisking motions of a rodent's vibrissae [5]. Similar to a skilled technician fine-tuning instruments, these deliberate motor activities prepare an organism's sensory systems to optimize the perception of specific stimuli types. This active orchestration and selective sensory data acquisition enhance an organism's understanding of its surroundings, enriching the sensory 'dialogue' between the organism and its environment [2, 6]. By meticulously exhibiting active sensing movements, animals obtain diverse and high-resolution information beyond what is achieved via passive reception of the sensory signals in the environment [7–9]. It is through these active sensing movements that animals achieve stable and precise navigation, engage in complex communication, and effectively utilize their habitat, ultimately enhancing their survival in diverse ecological niches [2, 10–12].

Active sensing is a sophisticated mechanism, involving purpose-driven movements. It is not simply a reactionary mechanism, but rather an intricate, intelligent interplay between the sensory and motor systems which seeks to adjust sensory inputs for enhanced perception. Translating this interaction into the "language" of engineering requires building closed-loop models, which encapsulate the processes' dynamism and responsiveness [12–14]. Within the proposed modeling frameworks, active sensing inputs act as disturbance signals, perturbing the motor commands generated by the task control. This is an intriguing paradox as despite often being orthogonal and even seemingly contrary to achieving task goals, active sensing movements improve state estimation, which in turn, improves task performance.

Active sensing manifests in various forms within the biological realm, each tailored to meet the specific needs of the species employing it. These processes can be categorized into distinct types, such as active illumination and active sensing through movement [2, 15]. Active illumination, observed in bats, involves transmission of a signal to the environment and interpretation of the resulting feedback. By analyzing the timing, direction, and frequency changes in the echoes, bats construct a detailed sensory representation of their surroundings, including the distance, shape, and location of objects [1, 10, 11]. Meanwhile, active sensing via movement is exemplified by the whisker movements in rodents. These small mammals continually adjust their whiskers in response to changes in their environment, thereby enabling spatial awareness and object detection [5, 16]. The diversity of active sensing is further exemplified by cockroaches, which utilize antenna movements to detect obstacles and gather tactile information [17, 18], spiders that interpret vibration signals transmitted through their webs for object localization [19, 20], and various animals that dynamically modify their sensory volume through adjustments in physical orientation and focus. By selectively fortifying their sensory inputs, these animals continuously reshape their interactions with the environment [21–24].

Weakly electric fish demonstrate a sophisticated approach to active sensing by employing both active illumination and active sensing through movement. Active illumination involves the use of electrosense, where these fish continuously emit an electric field and interpret the resulting feedback signals to construct a representation of their environment. The latter mechanism involves engaging in ancillary body movements, allowing them to modulate the sensory feedback received from the environment. Through these movements, they can fine-tune their electric perception to meet their specific needs. This paper focuses specifically on this second aspect of active sensing in weakly electric fish [1, 2, 7, 12, 21, 24].

In this paper, we explore various models of active sensing by movement in animals. One model we investigate is the open-loop model, which characterizes the active sensing signal generator in the central nervous system (CNS) as an open-loop noise source. Another model, recently published in the literature [25], is based on the stochastic resonance phenomenon observed in biological systems [26–28]. Different than open-loop models, this model–Biswas et al. (2023)–suggests introducing noise only when the state estimation performance falls below a certain threshold [25]. This model has two limitations. In this semi-closed-loop model, active sensing signals are triggered based on feedback from state variables, but the model does not proportionally adjust its noise output based on state-estimation performance. Our research challenges these traditional models with two distinct approaches. First, we explore the impact of mode switching in a new alternating model, which alternates between a tracking and active sensing controller based on the state estimation performance. However, both Biswas et al. (2023) and the proposed alternating model consider the active sensing signal as a white-noise signal with constant gain. Here,

we propose a novel closed-loop active sensing generator model, which continuously injects noise into the sensorimotor control process, inversely proportional to the state-estimation performance.

We examined the active sensing behavior of *Eigenmannia virescens*, a species of weakly electric fish, known for their preference to remain hidden within shelter-like structures in their natural habitats. Specifically, we focused on a unique behavior of these fish, termed refuge tracking, where they track the longitudinal movements of their refuge by swimming forward and backward along a single linear dimension [21, 29–33]. To study active sensing in *Eigenmannia*, we analyzed the kinematic responses of the fish during their unconstrained free refuge tracking behavior (see Fig. 1A). Our experimental setup involves a test aquarium with a 3D-printed refuge attached to a linear actuator. A computer-controlled system moves the refuge back and forth within the test setup, implementing predefined stimulus trajectories. The fish's behavioral kinematic responses are recorded using an NIR camera positioned beneath the test setup, capturing detailed information about their tracking response and any active sensing movements. These recorded data are utilized to develop a detailed closed-loop model that accurately captures the intricacies of the refuge tracking behavior and the active sensing mechanisms employed by weakly electric fish.

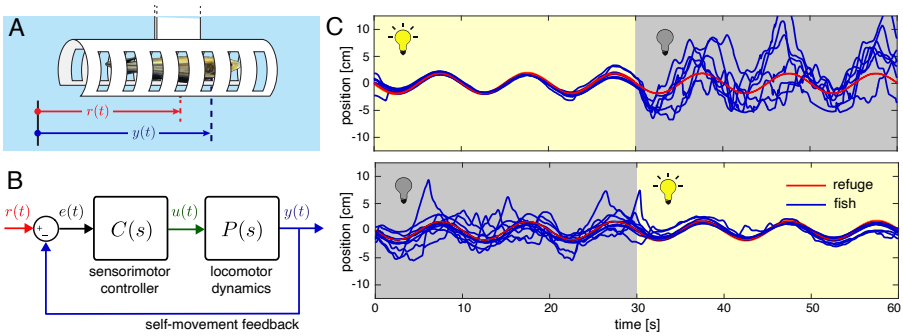

Fig. 1 (A) *Eigenmannia* tracking a refuge in which it is hiding. (B) A simple feedback control model of the refuge tracking behavior. (C) *Eigenmannia* exhibits high-frequency movements when swimming in the dark due to increased active sensing movements.

A vast majority of the literature [31, 34, 35] encapsulates the sensorimotor transformation–mapping from the sensory input to the motor commands–within a single sensorimotor controller unit (see Fig. 1B). However, these models, including our own previous work, fail to capture the active sensing movements exhibited by the fish, when the quality of the sensory information degrades. Fig. 1C illustrates two sample scenarios, where the illumination in the environment was changed either from light to dark or from dark to light. In light, *Eigenmannia* uses both visual and electrosensory systems to detect the relative movement of the refuge. However, in the dark, the fish dominantly relies on electrosensory cues due to the absence of light in the environment.

This substantial degradation in the quality of sensory information results in increased trial-to-trial variability for the same stimuli, validating the previous results of Stamper et al. (2012) [36].

The key contribution of this paper is the development of a comprehensive mathematical modeling framework that captures the sensorimotor control process employed by the fish during their refuge-tracking behavior. The proposed model encompasses an optimal controller for achieving the behavioral task, an active sensing generator model to drive ancillary body movements, and a state estimator for accurate estimation. This framework provides a versatile platform for exploring different active sensing models and allows for flexibility and adaptability for future research. To ensure the fidelity of our model and enable comparisons between different active sensing generator models, we performed a calibration step using actual fish data obtained during refuge tracking experiments. This calibration procedure enabled us to fine-tune the model parameters related to locomotor dynamics and the task controller, resulting in simulated fish movements that closely aligned with the trial-to-trial variability observed in real fish behavior. We applied the same approach to assess the predictive performance of various active sensing models for a fair comparison. Our findings demonstrate that the proposed active sensing generator model, which operates based on predictive state-estimation uncertainty, produces active sensing movements that are highly realistic and indistinguishable from the actual fish response. This model outperforms recent models in the literature, providing further evidence for the effectiveness of incorporating predictive uncertainty into active sensing modeling.

2 Results

2.1 A feedback control model of active sensing based on predictive covariance

We propose that active sensing behavior in weakly electric fish is intricately linked to the synergistic interactions between the sensory and locomotor systems. To characterize this coupling, we developed a new feedback control model by detailing the simple sensorimotor controller block used in the literature [31, 34, 35]. Fig. 2 illustrates the block-diagram representation of the proposed sensorimotor control model of the fish during refuge tracking.

We begin our modeling effort by choosing an appropriate "plant" dynamics corresponding to the swimming dynamics of the fish. Here, we use the linear, physics-based parametric model developed by Sefati et al. (2013) [37] as the "plant" in the form:

$$P(s) = \frac{k}{ms^2 + bs}. \tag{1}$$

Here, the parameters m, k, and b denote the mass, gain, and damping coefficients, respectively, while s encapsulates the complex frequency in the Laplace domain. In a follow-up work, this parametric model was validated using a

data-driven approach [35]. Therefore, we incorporate this swimming dynamics model as the "plant" in our sensorimotor control model of the fish.

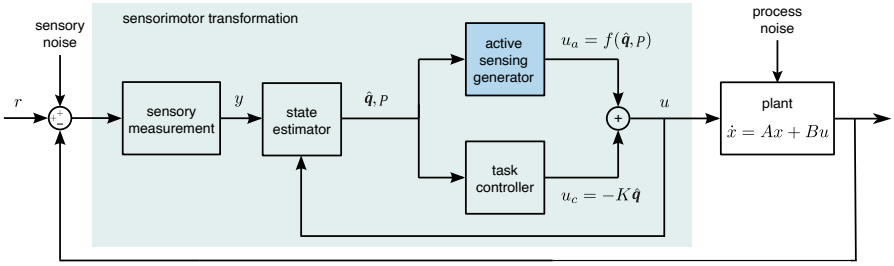

Fig. 2 The proposed feedback control model of the refuge tracking behavior. The relative movement of the refuge and the fish (contaminated by the sensory noise) is captured by the sensor model. The state estimator block estimates the internal states and associated covariance matrix using the efference copy. The task controller and active sensing generator use the state estimates and their covariance matrix to generate the motor commands. The plant, swimming dynamics of the fish, generates movement based on the given motor command.

The linear nature of the plant allows for the application of various control theory techniques. In this study, we implemented a state-feedback control policy for the task controller. We used pole placement to fine-tune the state-feedback gain in the task controller. A critical step in this approach is to calibrate the controller gain to closely match the closed-loop performance demonstrated by the fish in the light, where the fish needs minimal active sensing. This allows the segregation of the contributions of the task controller and the active sensing generator during light-deficit experiments. The formulation for the state-feedback task controller is as below

$$u_c(t) = -K\boldsymbol{q}(t) \ . \tag{2}$$

Here, K is the state-feedback gain, and the vector $\boldsymbol{q}$ is defined as $\boldsymbol{q} = \begin{bmatrix} p_q & v_q \end{bmatrix}^T$, where p_q and v_q denote the relative position and velocity between the refuge and the fish, respectively. See Methods for details.

The task controller, which works based on state feedback, requires an accurate estimation of the internal states of the system, such as the relative movement between the refuge and the fish. To remedy this, we adopted the electrosensory system model of the weakly electric fish developed by Kunapareddy et al. (2018) [38]. This sensory model was recently used by Biswas et al. (2023) [25] to develop an active sensing generator model for the weakly electric fish. A salient feature of this model is its ability to capture the behavior of certain biological sensors, such as the electroreceptors of the fish, using a nonlinear measurement function. Mathematically, this sensory model is in the form of

$$y(t) = ap_q(t)v_q(t) + bv_q(t) \ , \tag{3}$$

where a and b are parameters, describing the characteristics of the sensory scene around the fish. Note that as the velocity, $v_q \rightarrow 0$, the information associated with p_q disappears, rendering the system "unobservable". A detailed mathematical discussion about the observability issue for this sensory model can be found in [38]. Such a scenario underscores the inevitable need for the integration of active sensing strategies.

State estimation block plays a crucial role in making the sensory information derived from electroreceptors coherent and usable for the task controller. In other words, the state estimator works as a mapping from the sensory measurements to the neural representation of the sensory information. Due to the inherent nonlinearity of the sensor model, we employ the Extended Kalman Filter (EKF) as our state estimator structure. The EKF is well-suited to generate optimal state estimates given a nonlinearity either in the sensor or in the process model. By utilizing the EKF, we process and interpret the sensory measurements to obtain optimal state estimates and their covariance matrix, which will later be used for the task controller and the active sensing generator as depicted in Fig. 2.

A key point about the state estimators is that the accuracy of the state estimation depends critically on the observability of the associated states. One major drawback of the electrosensory model of weakly electric fish (see Eq. (3)) is that the system becomes unobservable when the speed of the relative motion between the refuge and the fish is close to zero (see [38] for a mathematical proof). Intuitionally, this is expected as the electrosensory system of these fish exhibits high-pass filtering characteristics–generates weak or no response when the sensory scene is at very low speeds or stationary. However, mathematically, this means that the system loses observability when the fish is close to perfect tracking. In this case, state estimation performance deteriorates, and the fish trajectories deviate from the refuge, as the performance of the state-feedback control depends on the quality of state estimation. The active sensing generator model helps to stabilize this relationship by injecting a purposeful disturbance to the motor commands.

The only remaining but the most crucial and novel part of the feedback control diagram is the active sensing generator block. Here, the active sensing generator works in parallel with the linear state-feedback task controller. The goal of the active sensing generator is to perturb the system to recover the observability. Thus, an ad-hoc model for the active sensing generator would be an open-loop noise source injecting noise into the system. However, the previous works clearly showed that animals adopt different stereotyped active sensing actions, whose form and strength vary depending on the quality of the sensory information [21, 39]. Motivated by the successful results of these works, we model the active sensing generator as a closed-loop regulator, which seeks to minimize the predictive uncertainty in state estimations. Therefore, our model consider active sensing generator as a purposeful control block rather than an open-loop noise source. To make the optimization more realistic, we

add two auxillary cost items to the active sensing generator model that penalizes the energetic costs and instantenous changes due to active sensing signal. Consequently, we formulate the cost function for the active sensing generator block as:

$$J(u_a) = \underbrace{\gamma_1 var(p_q)}_{\text{uncertainty}} + \underbrace{\gamma_2 u_a^2}_{\text{energetic cost}} + \underbrace{\gamma_3 \Delta u_a^2}_{\text{smoothness}} . \tag{4}$$

In our implementations, we used MATLAB's "fminbnd" optimization algorithm to determine the optimal active sensing input, u_a, for each iteration. Please see Fig. 3 for a block-diagram representation of the proposed optimization scheme.

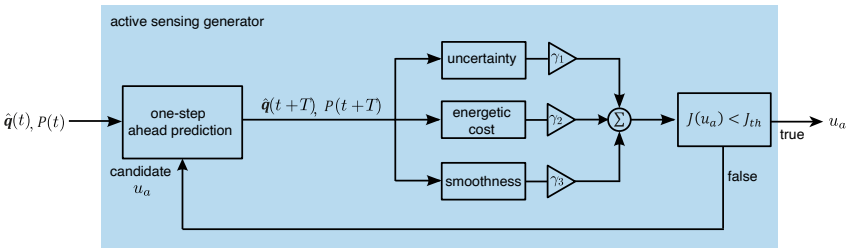

Fig. 3 Block diagram of the proposed active sensing generation method. This block is implemented as an optimization routine, which seeks to minimize the one-step ahead predictive covariance.

We use the predictive covariance in our cost function to take the optimal action for the next step. To achieve this, we use the posterior estimate of the covariance matrix provided by the EKF. This will be referred as "predictive uncertanity" matrix P for brevity. The P matrix quantifies the variance or uncertainty in fish's predictions about the sensory input, specifically the relative motion of the refuge and the fish. For each step, fish applies the optimal active sensing input, which minimizes the predictive uncertainty in its state estimation (see Eq. (4) for the full cost function). Note that a complete state vector may include the global position of the refuge and the fish to perform the simulations. However, some of these informations may not be available to the fish, for instance, fish can not infer the global position of the refuge but only its relative position to itself. Therefore, we only use the variance term associated to p_q, the relative motion of the refuge and the fish. The first cost term in Eq. (4) captures this aspect.

The efficiacy of the proposed simulation framework and the active sensing generator model is demonstrated in Fig. 4. Here, we segmented our simulations into four epochs to show different aspects of the active sensing phenomenon. In the first epoch, we bypassed the state estimator in Fig. 2 and directly fed the actual state estimates to the task controller. Note that this is not possible in a real life scenario, since the controllers can only access an estimate of the states based on sensory measurements. As expected, in this epoch, the fish model

performs accurate refuge tracking, perfectly matching the frequency, gain, and phase of the reference motion. However, the state estimator fails to infer the states as the system loses observability as the speed for the sensory error signal–difference between the refuge and fish– approaches zero. Besides, the variance of the state estimation increases substantially. In the second epoch, we keep using the actual states but add an active sensing signal, which seeks to minimize the predictive uncertainty in state estimations. Therefore, in the second epoch, we observe a drastic decrease in the variance of the state estimation error despite huge peaks in the magnitude of the state estimation error. This is mainly due to the fact that active sensing signals directly perturb the ideal tracking input as the task controller is using actual state information. The third epoch reflects the premise of the current paper, where the task controller uses state estimations and the active sensing generator seeks to improve the state estimation performance. In this epoch, both the magnitude and the variance of the state estimation error are diminished. This of course results in additional high-frequency oscillations in the tracking response of the fish. The last epoch shows how would the system respond if the active sensing generator is turned off, while the system uses estimated states to generate control signals. In this scenario, both the magnitude and variance of the state estimation error diverge. As a result, the model loses tracking of the refuge after a certain amount of time.

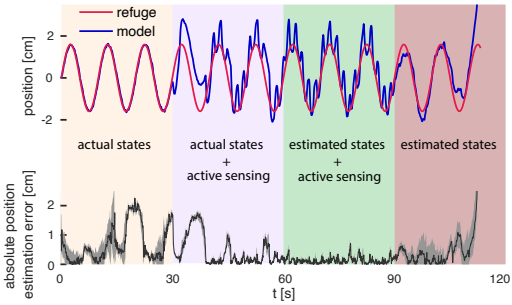

Fig. 4 Demonstrating the need for active sensing. The first epoch uses the actual states to achieve perfect tracking with substantial state estimation error. The second epoch adds active sensing inputs that improve the state estimation performance. However, feeding back the actual state as in these two epochs is not possible in real life. The third epoch uses estimated states and active sensing together, which is the ideal scenario. Here, the state estimation error is minimal and the model exhibits sufficiently good tracking. In the final epoch, we turn the active sensing off and the model quickly diverges from the reference as state estimation error increases.

2.1.1 Artificial Neural Network-Based Implementation of the Active Sensing Generator

The proposed active sensing generator model is supposed to work online and in real time to achieve the desired task performance. However, the optimization routine described in Fig. 3 may hinder potential real-life applications,

especially when the sampling period is too low. Moreover, we don't have any evidence for the neural implementation of such an optimization routine within the neural circuits of the central nervous system. The biological systems are optimal in various manners, however, we believe that this optimality is achieved through long experiences, which tunes the neural network to generate "optimal" outputs.

In our quest to understand the mechanisms behind the active sensing movements in weakly electric fish, we also examined the use of artificial neural networks (ANNs) to generate the "optimal" active sensing inputs that need to be injected into the system. To achieve this, we employed a feedforward neural network comprising 20 hidden neurons (illustrated in Fig. 5A) to capture the performance of the optimization routine described in Fig. 3. After a training period with the outputs of the optimization routine, the proposed ANN model achieved a great performance in replicating the outputs of the proposed optimization routine as illustrated in Fig. 5B. These findings emphasize the potential use of ANNs in studying the active sensing movements of biological systems. A more detailed discussion about the implementation of the ANN-based active sensing approach can be found in the Methods section. Note that one can strictly use an ANN-based approach to mimic the active sensing generator model in biological systems. However, the proposed parametric model is fundamental to understanding the underlying mechanisms governing the active sensing generation in these systems. Therefore, the entire analysis in this paper will use the intuitional optimization routine to study the roles of active sensing generator in the behavioral response of the fish.

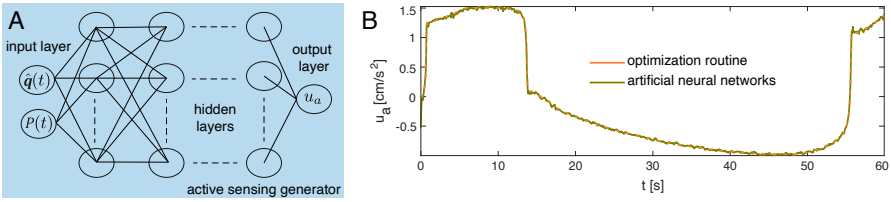

Fig. 5 (A) An artificial neural network implementation of the proposed optimization routine within our active sensing generator model. (B) The ANN-based implementation perfectly matches the output of the optimziation routine.

2.2 Weakly electric fish use predictive uncertainty to regulate its active sensing movements

Section 2.1 describes the details of our feedback control model that captures the contribution of active sensing in behavioral control. Our results showed that the proposed active sensing generator is successful in achieving the task objectives. Despite this success in terms of a design problem, our ultimate goal is not to achieve a perfect active sensing generator that guides the task controller. Instead, our goal is to show the predictive performance of the proposed active sensing generator and the associated feedback control system on actual

fish data. To achieve this, we conducted extensive computational analysis to validate the performance of the proposed model in predicting the behavior of the actual fish. The simulated feedback control model yields fish trajectories that are indistinguishable from actual fish movements.

To accurately quantify fish behavior, particularly in situations where active sensing movements are prominent, we conducted experiments on $N - 3$ fish under dim light conditions, specifically with illumination around 50 lux. During these experiments, we moved the refuge with a constant-frequency sinusoidal input of either 0.10 Hz, 0.15 Hz, or 0.25 Hz. Each experiment was repeated 10 times, and we recorded the trajectories of the fish in response to these stimuli. Detailed information about the experimental procedures can be found in the Methods section. The data obtained from these experiments played a critical role in the selection of parameters for our model, ensuring that it closely aligns with the observed behaviors of the fish.

As mentioned earlier, experiments conducted in well-illuminated conditions provided information for parameter selection in the task-level controller. However, for the identification of additional parameters related to active sensing generation, we focused on trials conducted in dim light conditions, where fish produce additional active sensing movements. These parameters that we estimate include scene parameters given in Eq. (3), measurement noise variances, and γ_i's in Eq. (4). To determine these parameter values, we performed a series of 10 trials involving a constant-frequency sinusoidal movement under dim light conditions. The discrepancies between this data and the outcomes of 1000 iterative simulations were assessed using the Maximum Mean Discrepancy (MMD) method, as described by Gretton et al. [40]. The MMD offers a reliable way to compare complex distributions without assuming any specific forms regarding the structure of the distribution. Subsequently, an optimization algorithm, outlined in the Methods sections, was applied to identify the optimal parameter set that minimizes the distance metric. This approach ensures that the model accurately replicates the observed behaviors.

Fig. 6 illustrates the simulation results of the proposed model after fitting the model parameters to the actual fish response. Fig. 6A shows the positional data of the fish from 10 different trials and the simulated fish position obtained through our proposed feedback control model. It is evident that the simulated fish closely replicates the actual fish's trajectory. The result of our predictive uncertainty model stays well within the trial-to-trial variability observed in actual fish.

Note that the trajectory of the simulated fish has some fast movements that deviate the trajectory of the fish from that of the refuge momentarily (see shaded areas in Fig. 6). These types of movements have also been reported in the literature, yielding a categorical behavior termed as *reset* [21]. Here, we investigated the underlying reason behind such instantaneous actions preferred by the fish and amazing also captured by our model. Fig. 6B-C depicts the active sensing generator output and the state estimation error along with its variance. Note that these fast movements occur when the active sensing

generator undergoes a sudden change. Mathematically, our cost function that is given in Eq. (4) aims to prevent such sudden changes in the output of the active sensing generator based on its relative weight in the overall cost. However, the increased variance in the state estimation overcomes the weight of smoothness after a certain threshold, yielding another optimal solution that can only be achieved with a sudden change in the control action. Note that the model experiences increased uncertainty in the state estimation error apriori to these sudden control actions. One could argue that we can simply eliminate the smoothness criteria that we have in our cost function to obtain a better tracking result. However, as stated earlier, our goal is to find the best model that captures the actual fish behavior.

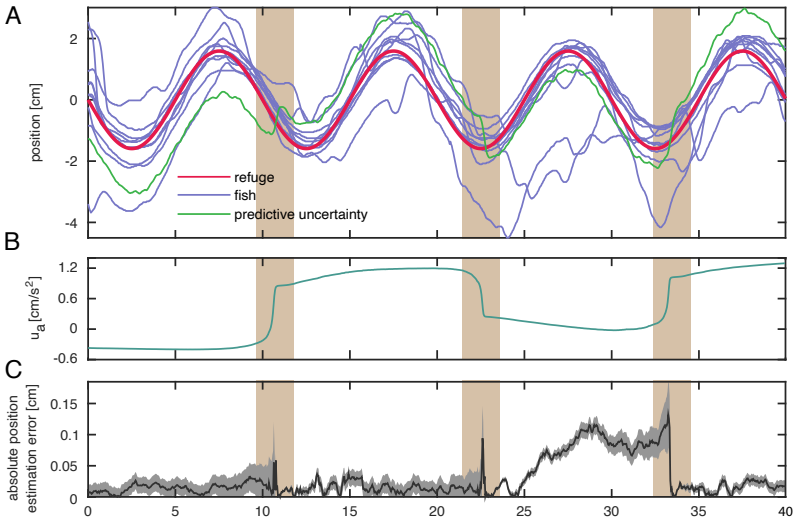

Fig. 6 Model vs. fish. (A) The trajectories (10 replicates) of an actual fish tracking a refuge moving at 0.1 Hz and the response of the proposed predictive uncertainty model. (B) The output of the active sensing generator for the proposed model. (C) State estimation error and associated variance term depicting the quality of the state-estimation for the proposed model.

The time domain plots in Fig. 6 are good for having an intuitional understanding of how the proposed model, and hence the active sensing mechanism in fish, work. However, it is quite difficult to quantify the predictive power of the proposed model in terms of capturing the details of the actual fish movements. Besides, the periodic nature of the input–output signals motivates us to perform the quantitative analysis in the frequency domain.

Fig. 7 presents a complete frequency domain view of an actual fish's data and the results of the proposed model. Here, we use the Discrete Fourier Transform of the actual time-domain data from the fish to generate a confidence interval reflecting the trial-to-trial variability of the actual fish. We used the results from the 10 replicates to generate 95% confidence intervals for each test

frequency. We also report the mean response of the simulated fish obtained from 1000 random realizations of the stochastic model parameters such as process and measurement noise. Our results show that for all three test frequencies, the results of the proposed model fall within the confidence interval of the actual fish except for a few exceptional frequencies which we do not stimulate the fish at. We will provide further statistical analysis and compare our approach with other methodologies in the literature in the following section.

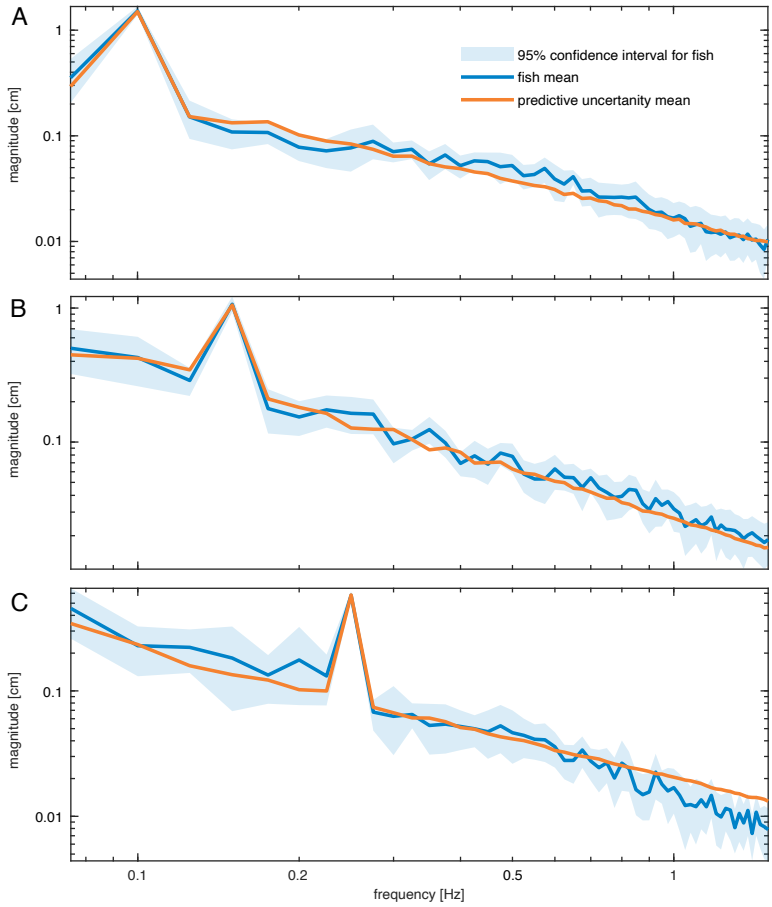

Fig. 7 The frequency domain responses of the fish and our model at (A) 0.1 Hz, (B) 0.15 Hz, and (C) 0.25 Hz. The blue-shaded region represents the bootstrap confidence intervals for the mean of the fish response, capturing the %95 range. The solid blue line is the mean response of the fish for the 10 replicate trials for each frequency. The solid orange line represents the mean of our model's outputs, obtained from 1000 random realizations. The response of the proposed model lies within the confidence interval of the actual fish, suggesting that it is indistinguishable from the data of the actual fish.

2.3 Active sensing is a closed-loop phenomenon

This section aims to conduct a comparative analysis of the predictive performance of the proposed model. One simple explanation for generating active sensing movements is to introduce an open-loop noise signal that perturbs the system dynamics, enabling observation of the states for state estimation. It is possible that open-loop noise generator models may be sufficient for accurate state estimation and successful tracking. The simulation framework we've developed allows the implementation of this model as well with a minor tweak in the block diagram depicted in Fig. 2. In the case of an open-loop model, the active sensing generator block does not require any input from the state estimator. Instead, it pumps in a Gaussian white noise signal as a disturbance to the output of the task controller. The strength of the open-loop noise signal is tuned to obtain an optimal fit to the response of the actual fish for a fair comparison. Here, we evaluate if the open-loop model can capture the active sensing movements observed in actual fish based on same system identification procedure in the previous section.

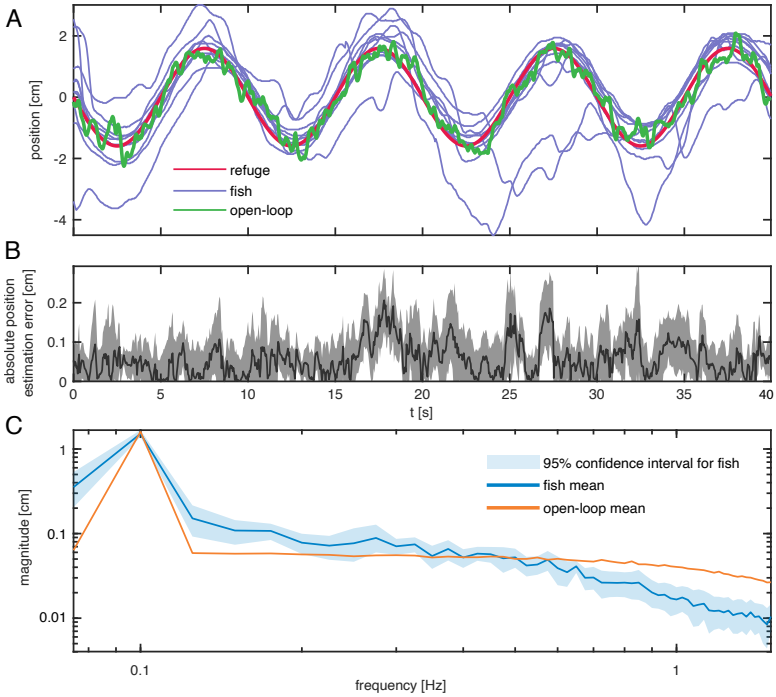

Fig. 8 Open-loop model vs. fish. (A) The trajectories (10 replicates) of an actual fish tracking a refuge at 0.1 Hz and the response of the open-loop active sensing generator model. (B) The state-estimation error and the associated variance term show the quality of the state estimation. (C) The frequency domain response of the fish with 95% confidence interval and the mean response of the simulation model with an open-loop active sensing generator.

Fig. 8 shows the results of our comprehensive analysis with the open-loop active sensing generator model. In Fig. 8A, we report the time-domain trajectories of the actual fish, obtained from 10 replicated trials as well as the response of the simulated feedback control model with the open-loop active sensing generator. The addition of an open-loop noise signal to the task controller yields noisy oscillations modulated by the low-frequency tracking signal at the stimulus frequency. Fig. 8B shows the corresponding state estimation error and variance, quantifying the state-estimation performance. The open-loop model yields considerably less state estimation error as compared to no active sensing scenario presented in the last epoch of Fig. 4. However, the state-estimation error and associated variances are quite high as compared to the results of the predictive uncertainty method that we've proposed in this paper (see Fig. 6). Finally, Fig. 8C shows the frequency response plots of the actual fish with 95% confidence interval and the response of the feedback control model based on an open-loop active sensing generator. The key result here is that the responses due to the open-loop model do not fit well into the trial-to-trial variability observed in real fish despite its successful tracking performance in the time domain. Therefore, the predictive capabilities of the open-loop active sensing generator model are not sufficient enough to capture the details of the actual fish movements.

Additionally, we compare our findings to a recent model proposed by Biswas et al. (2023) [25], which describes active sensing movements in these fish (see Fig. 9). This approach is primarily based on a different application of the stochastic resonance phenomenon, which is observed in both biology and engineering. Unlike open-loop models, Biswas et al. (2023) employ a semi-closed-loop model that activates the active sensing generation signal only when the state estimation performance falls below a certain threshold, and deactivates when it surpasses another threshold [25]. In this model, the amount of active sensing input injected into the system is independent of the system's states, but it is triggered based on the state variables, creating a loose dependence on feedback. The simulation framework we've developed allows the implementation of this model as well with minor modifications of the block diagram depicted in Fig. 2. The application of Biswas et al. (2023) requires the addition of a switch in front of the active sensing generator block, which either enables the injection of an open-loop noise into the control loop or eliminates the contribution of the active sensing generator. For a fair comparison, we estimated the three decision parameters used in Biswas et al. (2023) [25] that specify the active sensing generator, such that the model fits best to the actual fish data. Specifically, these parameters are the standard deviation of the Gaussian white noise signal, and the upper and lower thresholds on state-estimation performance to switch from active sensing to no active sensing. Note that Biswas et al. (2023) studied active sensing within the context of a stabilization task, where the refuge is stationary. In our scenario, we utilize this model within the context of a tracking task, where the reference input (refuge position) is dynamically changing.

Fig. 9 shows the results of our comprehensive analysis with the active sensing generator model of Biswas et al. (2023). The time-domain data presented in Fig. 9A shows that this model also achieves a sufficiently good tracking performance with extra high-frequency oscillations around the stimulus trajectory. Note that Biswas et al. (2023) differs from the open-loop model in the sense that it can switch off the active sensing generator. The durations, where the model switches off the active sensing generator are shaded in gray. Fig. 9B shows the corresponding state estimation error and variance, quantifying the state-estimation performance. The performance is comparable to the open-loop case as Biswas et al. (2023) approximates the open-loop model as the duration of the shaded regions approaches zero. Fig. 9C illustrates the frequency response distribution of the actual fish vs. Biswas et al. (2023). Note that this model also does not generate frequency responses that lie within the trial-to-trial variability of the actual fish.

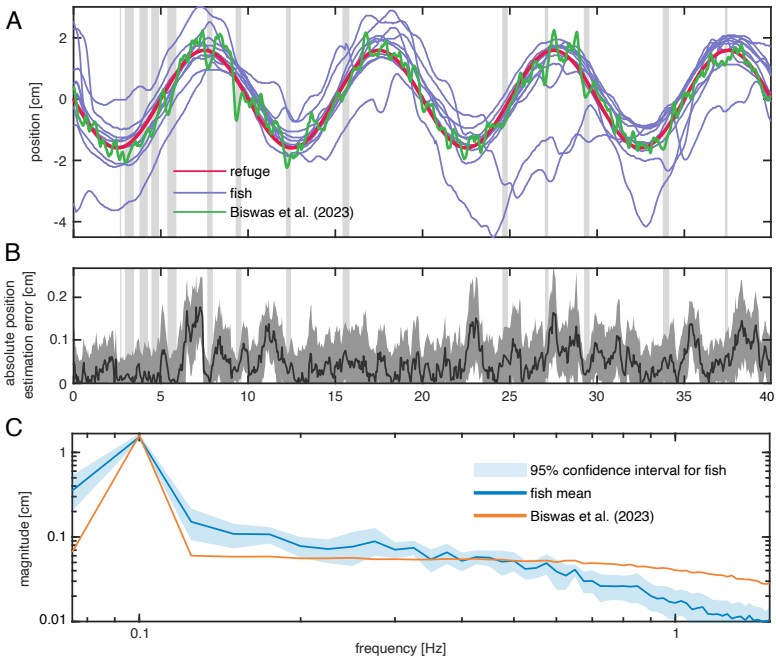

Fig. 9 Biswas et al. (2023) [25] vs. fish. (A) The trajectories (10 replicates) of an actual fish tracking a refuge at 0.1 Hz and the response of the active sensing generator model of Biswas et al. (2023). (B) The state-estimation error and the associated variance term show the quality of the state estimation. (C) The frequency domain response of the fish with 95% confidence interval and the mean response of the simulation model with the active sensing generator model of Biswas et al. (2023).

A fundamental issue both with the open-loop model and Biswas et al. (2023) is that they both add a Gaussian white noise signal on top of the task controller output. Note that these noise signals appear as a constant line across

the frequency axis since they have identical power at each frequency. Therefore, the addition of such noise profiles can only elevate the magnitude plot of the frequency response of the task controller. This is why we see a nearly flat line beyond the stimulus frequency. This is one of the primary reasons why these models can not capture the frequency response characteristics of the actual fish, which have a decreasing power distribution beyond the stimulus frequency. We anticipate two alternative approaches to remedy the inherent problem with these models. First, one can choose a different strength gain for each active sensing epoch. Specifically, the strength of the noise can vary across time to shape the frequency distribution of the contribution of the active sensing input. This approach adds one more degree of freedom to the active sensing generator to fit the actual fish data. However, this results in more complex models with overfitting issues. Secondly, we can reshape the overall frequency response by swapping between the active sensing generator and the task controller based on the state-estimation performance. The motivation here is that the task controller generates a control action based on a weighted sum of the estimated states. Therefore, it is not helpful to use the task controller when the state estimation performance is poor. Therefore, we modify the approach of Biswas et al. (2023) to alternate between the task controller and the active sensing generator based on the quality of the state estimation. In this scenario, the simulation model uses the task controller when the state estimation performance is acceptable. Otherwise, we switch off the task controller and alternate to the active sensing generator to quickly recover the state estimation performance.

Fig. 10 shows the results of our comprehensive analysis with the alternating controller model extended upon Biswas et al. (2023). Fig. 10A shows a successful tracking performance with frequent switches between the task controller and the active sensing generator. As anticipated, when the state estimation performance is poor, the system switches to active sensing and quickly recovers. This is why we observe frequent but short active sensing epochs, illustrated with gray shaded regions in Fig. 10A-B. Note that the estimation performance, especially variance is low in Fig. 10B as the control model switches to active sensing as soon as the overall state estimation quality drops below a certain threshold. Fig. 10B illustrates the frequency response distribution of the actual fish vs. Biswas et al. (2023). Note that this model also does not generate frequency responses that lie within the trial-to-trial variability of the actual fish. Fig. 10C shows the frequency response distribution of the alternating mode model. Despite discrepancies, the alternating mode model exhibits very close performance with respect to the trial-to-trial variability of the fish.

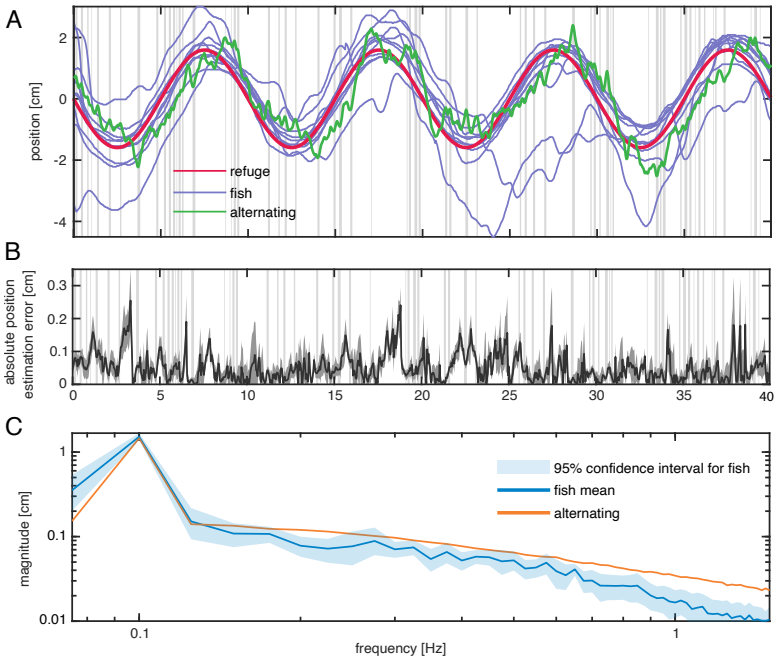

Fig. 10 Alternating mode model vs. fish. (A) The trajectories (10 replicates) of an actual fish tracking a refuge at 0.1 Hz and the response of the alternating active sensing generator model. (B) The state-estimation error and the associated variance term show the quality of the state estimation. (C) The frequency domain response of the fish with 95% confidence interval and the mean response of the simulation model with the alternating active sensing generator model.

We also performed a comparative analysis for the four methods mentioned in this paper across all $N = 3$ fish and at the free stimulation frequencies used in the actual experiments. For a fair comparison, we fit the model parameters for each case to yield its optimal output in terms of explaining the actual data. We used the same metric in the identification of active sensing movement to quantify the difference between frequency response distributions of the actual experiments and the model predictions with their own optimal parameters.

Fig. 11 illustrates the MMD scores of the four methods across all fish and test frequencies. In all fish and almost at all frequencies, the proposed predictive covariance method yields the minimum MMD score, suggesting that the frequency distribution is closest to the actual fish data among the four models. Open-loop model and Biswas et al. (2023) yield very similar results in all scenarios. The alternating mode model shows close performance to the predictive uncertainty method.

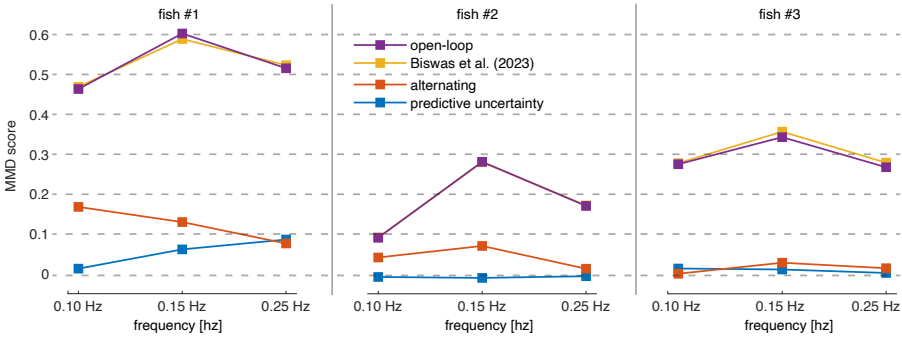

Fig. 11 MMD values for the four models for all three fish and the three test frequencies.

The MMD test is very useful in terms of comparing the distance of distributions. However, we also performed a p-test to assess if there was a statistical difference between the predicted and actual frequency responses. The null hypothesis suggests that there is no statistical significance between the two distributions. Therefore, a p score less than 0.05 rejects the null hypothesis, suggesting that the two distributions are statistically different. In the case of system identification, we expect to find p-values higher than 0.05 to state that there is statistical significance between the actual and predicted distributions.

Table 1 Comparison of p-values for all four models and the actual response of the fish. The cases with $p > 0.05$ are marked with a star to indicate that there is no statistical significance between the model predictions and the actual data.

		predictive uncertainty	alternating	Biswas et al. (2023)	open-loop
Fish 1	0.10 Hz	0.26⋆	2e-3	0.00	0.00
	0.15 Hz	0.09⋆	2e-3	0.00	0.00
	0.25 Hz	0.05⋆	0.06⋆	0.00	0.00
Fish 2	0.10 Hz	0.63⋆	3e-3	0.00	0.00
	0.15 Hz	0.60⋆	0.01	0.00	0.00
	0.25 Hz	0.46⋆	0.09⋆	0.00	0.00
Fish 3	0.10 Hz	0.18⋆	0.40⋆	0.00	0.00
	0.15 Hz	0.20⋆	0.09⋆	0.00	0.00
	0.25 Hz	0.36⋆	0.17⋆	0.00	0.00

Table 1 lists the p-values for all four models for all three fish and the three test frequencies. Biswas et al. (2023) and the open-loop model predictions yield distributions with $p < 10^{-16}$, the numerical resolution of Matlab. This suggests that both of these methods reject the null hypothesis in all scenarios. In other words, there is a statistically significant difference between the frequency response distributions of these two models and the actual fish data despite fitting their parameters to obtain the optimal results–minimum MMD. The alternating mode model, which we proposed as an interim model

between Biswas et al. (2023) and predictive uncertainty yields higher p values, suggesting that it is capable of generating distributions very close to that of the actual fish in most cases. However, the proposed predictive uncertainty model produces frequency response distributions that have no statistical significance as compared to the frequency response distribution of the actual fish in all scenarios.

Note that here we used all the data during the parameter estimation process. Therefore, there is a chance of overfitting the data. To avoid this, we conducted cross-validation to reveal if the model performs similarly on test data, which was not used during the parameter identification procedure. We performed cross-validation only on the proposed predictive uncertainty model as the other methods already resulted in statistical significance despite training them on all of the data.

Table 1 shows a summary of the 3-fold cross-validation results of the predictive uncertainty model. Here, the training and test sets are divided to include nearly equal amounts of data from all frequencies. Note that in all test cases, the proposed model generates distributions with $p > 0.05$, suggesting that there is no statistical significance between the model predictions and the actual fish data, even if the data is completely novel to the model. In terms of the training sets, there is only one scenario, specifically in fold #3 of fish #1. It is highly likely that an outlier in this fish causes a statistical significance between the model predictions and the actual fish response.

Table 2 3-fold cross-validation results of the predictive uncertainty model.

	Fish 1				Fish 2				Fish 3			
	test		training		test		training		test		training	
	MMD	p value	MMD	p value	MMD	p value	MMD	p value	MMD	p value	MMD	p value
fold 1	0.05	0.15	0.05	0.05	0.00	0.59	0.00	0.54	0.00	0.39	0.00	0.45
fold 2	0.05	0.14	0.03	0.11	0.00	0.56	0.00	0.52	0.00	0.37	0.00	0.32
fold 3	0.02	0.26	0.05	0.04	0.00	0.52	0.00	0.64	0.00	0.54	0.00	0.31

3 Discussion

3.1 Making the Most of Sensory–Motor Coupling Through Active Sensing

In control theory, the separation principle stands as a pivotal concept, enabling engineers to independently design observers and controllers within a feedback control system. Nevertheless, in the context of biological systems, notably in animals, a recurrent departure from this principle is evident. This deviation arises due to the inherent interplay between motor actions and sensory signals,

whereby the actions of the organism directly influence the sensory information it receives from the environment. Remarkably, animals benefit from this intrinsic coupling to improve behavioral task performance. Animals engage in ancillary motor actions that alter the spatiotemporal characteristics of the sensory information they perceive from the environment. Such purposeful motor actions are termed active sensing movements. Animals employ active sensing movements to best utilize the coupling between their sensory and motor systems.

This link between motor and sensory processes poses a significant challenge in the study and engineering of biological control systems. Embracing and comprehending these violations of separability holds profound implications for advancing our understanding of biological systems, unveiling insights that could potentially influence fields such as biology and robotics by shedding light on the exceptional adaptability and resilience exhibited by living organisms. In this paper, we proposed a mathematical framework that adeptly captures and models the intricate interplay between motor actions and sensory signals, in biological control systems, specifically for the weakly electric fish.

While manifold forms of active sensing movements pervade animal behavior, full comprehension of the dynamics underpinning these movements continues to evade researchers [5, 22, 23]. A prevalent hypothesis suggests that active sensing operates akin to an open-loop system where process noise, or a population of active sensing neurons, introduces broad-spectrum disruptions to the motor commands [41]. However, evidence of active sensing movements explicitly attuned to the specific behaviors in animals challenges this notion [42]. Consider, for example, the minute motoric adjustments made by our fingers to decode the texture of a surface or the distinctive lift-and-shift motion used to deduce an object's weight; these purposeful actions extend beyond occurrences attributable to random noise interference.

We propose an alternative hypothesis suggesting that active sensing movements are finely tuned to the specific needs of the behavioral task. We contend that active sensing movements are continuously regulated by the central nervous system to match the spatiotemporal characteristics of sensory information with the optimal operating regime of the associated sensory receptors and neural circuits. This perspective recognizes active sensing movements as purposeful adaptations, meticulously designed to maximize the effective processing of sensory information. It supports a refined understanding of the architecture and adaptability of biological control systems, carrying ramifications for numerous fields including neuroscience, robotics, and artificial intelligence [43–46].

In accordance with the outlined parameters above, this study manifested an exhaustive feedback control model, shedding light on the distinct characteristics innate to the refuge-tracking behavior in weakly electric fish. From establishing a foundation on the fish's electrosensory system, the model meticulously traced the full range of the kinematic process, culminating in capturing the motion dynamics of the fish.

Our approach predominantly concentrated on the electrosensory system of the fish, consciously sidestepping the unexplored complexities and the elusive dynamics of multisensory integration processes. Our model assimilated key features from existing literature studies of the electrosensory system, predominantly incorporating the integral concept of a high-pass filter characteristic [38]. Consequently, the creation of a state estimator ensued, utilizing the capabilities of an Extended Kalman Filter (EKF). We conceived the fish's task controller as an optimal state-feedback controller. Simultaneously, we constructed an active sensing generator designed to produce active sensing inputs, serving as a disturbance factor to the output of the task controller. This inventive active sensing generator operates under the guiding principle of minimizing uncertainty in the state estimation for the forthcoming cycle. Ultimately, the merging of these motor commands ensues, aligning with the swimming dynamics of the fish. This adopted a model previously validated and recognized in the literature [35, 37].

A significant point that warrants emphasis is the execution of exhaustive optimization iterations to align the model parameters to the experimentally collected data from the fish. This step was instrumental in bridging the theoretical mathematical model to the tangible, biological subject of the study. The methodology employed, the subsequent data, and the resulting analysis could set a precedent for similar multidimensional, dynamic models in future research avenues.

3.2 How Can a Biological System Implement Predictive Uncertainty Based Active Sensing?

The human body possesses a wide range of potential movements, yet we tend to exhibit stereotypical motion patterns for specific tasks. This is because each movement carries a certain cost, and our brains strive to minimize this cost when selecting the most suitable movement. According to optimal control theory, this cost comprises external goals such as accuracy and regularization costs like smoothness. During movement, the brain utilizes sensory information to determine the next motor output, resulting in optimal feedback control. However, previous models have overlooked the dependence of sensory information on motor feedback. Yeo et al. proposed that movement planning should also consider the influence of movement on sensory feedback. Although this approach may result in less optimal movements in terms of accuracy and energy efficiency, it can enhance the quality of sensory information and improve movement precision. To address this, they developed an optimal feedback control framework that incorporates state-dependent sensory noise. Through experimental manipulation of this noise, they demonstrate that humans can develop sensorimotor strategies to reduce overall cost, which aligns with their proposed model [47].

The proposed predictive uncertainty-based active sensing generator model requires the solution of a complex optimization problem, which is implemented in Matlab using particle swarm optimization. However, we do not expect a

biological system to solve the optimization problem in this manner. Biological systems learn by experience and tune their neural circuity to reflect the outcomes of this learning process. In engineering terms, biological systems have a well-trained neural network, which continuously improves with the new information, that instantaneously generates optimal control outputs. We showed that it is indeed possible to train an artificial neural network (ANNs) that matches the output of the complex optimization routine that we are currently implementing. The key disadvantage of an ANNs-based implementation is that the neural networks do not provide insight into the underlying mechanistic principles of active sensing. Therefore, we use the optimization routine in our implementations but we show that an ANN-based implementation would yield the same results instantaneously without needing to solve the optimization problem.

3.3 Predictive Uncertainty Model Generate Statistically Indistinguishable Distributions Unlike Other Models

The comparative analysis between the four active sensing generation models can be analyzed from two perspectives. In terms of a design problem, the open-loop model generates the most desirable tracking response as the simulated fish can accurately track the low-frequency stimulus with some extra high-frequency oscillations. This is clear from the time-domain responses presented in Fig. 8. However, the primary goal of modeling the active sensing behavior in weakly electric fish is to find the best model that captures the characteristics we observed in actual fish. Therefore, in terms of a system identification problem, the open-loop model seems to be the worst-performing model that captures the frequency domain characteristics of the actual fish.

We used a p-test to evaluate if the frequency response distributions of the models have statistical significance against the frequency response distribution of the actual fish. Our results reveal that only the predictive uncertainty model that we proposed in this paper generates trajectories that have statistically indistinguishable trajectories for all cases among the four models we used in our comparative analysis.

In general, frequency domain analyses do not capture some salient features of fish's tracking behavior. For instance, the power at a frequency is technically the cumulative sum of the movement at that frequency across time. In other words, the information about the timing of events is lost during the frequency domain analysis. This is why the proposed models can not reproduce the exact time trajectories of the actual fish experiments. The key point here is that the fish itself can not also replicate the same trial due to variability in their responses. Our goal is to ensure that the model predictions stay well within the trial-to-trial variability of the actual fish responses.

3.4 Diagnostic Potential and Insights into Sensory Processing in Neurodevelopmental Disorders

The practical implications of active sensing extend beyond theoretical consequences. It has been observed that individuals with conditions such as autism, schizophrenia, and attention-deficit/hyperactivity disorder (ADHD) exhibit impaired entrainment to visual or auditory stimuli. These impairments are associated with abnormalities in the neural network responsible for active exploration, involving various cortical and subcortical areas associated with specialized functions. Disruptions in this network can result in specific disturbances in active sensing dynamics, such as preparing and executing eye movements and integrating information across saccades. Consequently, these disruptions can potentially serve as diagnostic indicators. For instance, infants who are later diagnosed with autism spectrum disorders tend to focus less on the eyes when viewing faces, while children with dyslexia display alterations in their fixation patterns even before experiencing reading difficulties. Patients with Alzheimer's disease and mild cognitive impairment exhibit impaired visual search patterns, and individuals with Parkinson's disease tend to have prolonged fixations when visually exploring complex images. These findings suggest that neurodevelopmental disorders selectively and specifically affect active sensing behavior, indicating early disturbances in the visual and oculomotor systems that alter visual sampling behavior [6, 48].

Certain models propose a unified understanding of active sensing, suggesting that modulations in whisker movements serve as an overt expression of the animal's changing focus of attention. This perspective enhances our comprehension of the whisker sensory system and provides insights into attention management in these animals [6, 12, 49].

Traditionally, biological sensors such as the eyes and fingertips have been regarded as passive, merely converting input energy into neural signals. However, a closer examination of how humans and animals gather information reveals that it is an active sensing process. For instance, we actively use our fingers to touch and manipulate objects, rather than waiting for something to touch our hand. Similarly, when we view our surroundings, we actively move our eyes to systematically sample the scene through eye movements. This paradigm indicates that a substantial portion of sensory input entering the brain is actively obtained through motor sampling. The motor control of sensory input has significant implications for understanding sensory processing. Attention plays a pivotal role in active sensing by enhancing relevant input and disregarding irrelevant stimuli. Although attention and motor sampling can be dissociated, as attention can operate without overt motor activity or be directed to a different location than where the sensors are aligned, in natural active sensing, attention rarely occurs without any associated motor routine.

3.5 Navigating Complexity in Active Sensing: Contrasting Engineering and Nature's Innovations

The field of engineering has extensively explored active sensing, showcasing its effectiveness through numerous working examples. Engineers have successfully utilized active sensing principles to design and optimize various systems. However, one may argue that the intricacies of active sensing are not always necessary in engineering. The advent of advanced sensors and sophisticated technologies allows many engineering challenges to be tackled without resorting to the complexities of active sensing. These high-precision and reliable sensors often suffice for fulfilling the required tasks.

Conversely, it is important to recognize that organisms in nature, such as the weakly electric fish, heavily rely on innate mechanisms like active sensing to navigate and interact with their environment. This contrast between engineering and nature emphasizes the adaptability of natural systems and the innovative solutions they have developed over time. While engineering has the advantage of external tools and technologies, nature has evolved to efficiently utilize active sensing as an integral part of survival.

The principle of Occam's razor advocates for favoring simplicity when competing hypotheses yield the same predictions. However, as we explore the intricate world of weakly electric fish behavior, we realize that increasing complexity in our models is not merely a choice but often a necessity. While simplicity has its appeal and elegance, it may not capture the full spectrum of observed phenomena in nature. In the case of the weakly electric fish, a basic model falls short of adequately explaining their active sensing behavior. This limitation not only hinders our understanding of their behavior but also limits progress in exploring more advanced aspects, such as the underlying neural mechanisms. Hence, while simplicity is valued, we must embrace complexity when it provides a more comprehensive and accurate representation of reality.

4 Methods

4.1 Experimental Setup

We constructed a unique experimental setup for this study, resembling a specialized aquarium where the fish engage in tracking behavior within a moving PLA (polylactic acid) refuge. The refuge's movement is controlled by a high-precision, single-axis linear actuator system powered by a Maxon DC motor. A section measuring 25 $cm \times 50$ cm at the base of the fish test area was replaced with glass to facilitate the capture of accurate, high-quality, bottom-view images using a Near-Infrared (NIR) Basler camera positioned underneath the setup.

Our system's electronic and software architecture runs on the Robot Operating System (ROS). System operations are performed in (nearly) real-time with an online loop frequency of 25 Hz. The system's main software runs on an

Nvidia Jetson NX card employing the ROS operating system. The Nvidia Jetson board is responsible for executing tasks, including initiating and managing the relevant experiment sequence based on user interface commands, delivering necessary motion commands to the motor driver, and processing feedback about the positions of the motor and the fish. Maxon EPOS4 motor driver controls the motion of the linear actuator system based on the commands received from the Nvidia Jetson NX board. The trajectories of the fish are generated by tracking the fish movements from camera records using template matching.

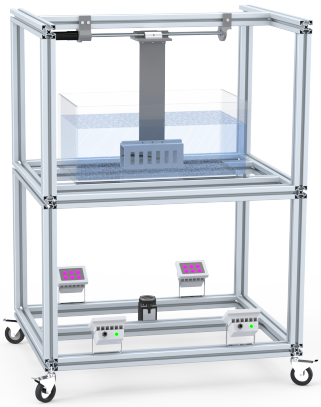

Fig. 12 Experimental setup

4.2 Experiment Procedure

This study employed three individual weakly electric fish (*Eigenmannia virescens*), aged between 18 and 24 months, to perform refuge tracking experiments. All experiments were conducted in compliance with the guidelines set by the Hacettepe University Animal Experiments Ethics Committee. Throughout the experiments, the water temperature and pH values were stringently maintained at 25 $\pm 1°C$ and 7.2, respectively. The fish were nourished daily with frozen blood worms.

Our research prioritized ethical practices with a focus on minimizing stress on the fish. We did not differentiate between male and female fish used in our trials and ensured no harm was caused to any fish. Prior to initiating any experiment, we allowed an acclimatization period of 2 to 24 hours, where the fish remained in the experimental setup.

The experiments were performed under light (300 lux) and dim light ($\approx$ 50 lux) conditions alongside low conductivity (roughly 40 mS). Our PLA refuge, measuring 14 cm in length and 4 cm in width, with windows, was

utilized for the testing. The refuge was moved with a single constant-frequency sinusoidal input at 0.10 Hz, 0.15 Hz, or 0.25 Hz.

Each fish experienced a series of ten repeated trials, each lasting one minute (equivalent to 1500 frames). For analyzing the trials, the fish's fore-aft position was tracked from recorded video using an open-source Python code.

4.3 Simulation

4.3.1 Plant Modeling and Dynamics

As mentioned earlier, the physics-based parametric model introduced by Sefati et al. [37] provides a comprehensive framework for characterizing the locomotion behavior of weakly electric fish. Following the established methodology in the field, we adopt the linear musculoskeletal plant in the form of Eq. (1) for our simulation and identification environment as the "plant" in Fig. 2.

Uyanik et al. [35] provide empirical evidence underscoring that while there is inherent and relatively high variation in parameter values within the equation Eq. (1) among individual fish, there exists a noteworthy consistency in closed-loop performance across different fish. Moreover, they show the resilience of closed-loop performance to mismatches between the plant and controller components by swapping controllers and plants among individuals. This compelling finding suggests that, with the establishment of a robust feedback mechanism, cross-utilization of plant parameters from one fish to another is feasible. Building on these insights, our study adopts the parameter values detailed in [35], specifically $m = 0.0025;\ kg$, $k = 0.2385;\ N/m$, and $b = 0.0269;\ Ns/m$. We use these values as a foundational reference for our analysis, with a focus on understanding the closed-loop performance of the fish under dim-light conditions, which we will discuss in the subsequent section.

Describing the fish's state through its position and velocity, represented as $\boldsymbol{x} = \begin{bmatrix} p_x & v_x \end{bmatrix}^T$, and making use of equation Eq. (1), we can formulate the state-space representation of the plant dynamics as

$$\dot{\boldsymbol{x}}(t) = \underbrace{\begin{bmatrix} 0 & 1 \\ 0 & -b/m \end{bmatrix}}_{\mathrm{A_f}} \boldsymbol{x}(t) + \underbrace{\begin{bmatrix} 0 \\ k/m \end{bmatrix}}_{\mathrm{B_f}} u(t). \tag{5}$$

Subsequently, we discretize these continuous equations using a sampling interval of $T = 0.04\ s$ to facilitate discrete-time data acquisition, simulation, and estimator/active sensing formulation. This discrete model accounts for the intrinsic dynamics of the fish while also incorporating the process noise ω:

$$\boldsymbol{x}\left((k+1)T\right) = A_f \boldsymbol{x}(kT) + B_f \left(u(kT) + \omega(kT)\right), \tag{6}$$

where we assume that process noise is in the form of a zero-mean Gaussian distribution with a standard deviation of σ_w, i.e. $\omega \sim \mathcal{N}(0, \sigma_w^2)$.

The representation of the fish's pursued refuge, i.e. reference signal, is modeled employing a constant velocity model, a commonly accepted framework in external target tracking applications [50–52]. The refuge state, encapsulating its position and velocity, is denoted as $\boldsymbol{r} = \begin{bmatrix} p_r & v_r \end{bmatrix}^T$. In this paradigm, the dynamic evolution of the refuge system is characterized by:

$$\boldsymbol{r}\left((k+1)T\right) = \underbrace{\begin{bmatrix} 1 & T \\ 0 & 1 \end{bmatrix}}_{\mathrm{A_r}} \boldsymbol{r}(kT) + \underbrace{\begin{bmatrix} T^2/2 \\ T \end{bmatrix}}_{\mathrm{B_r}} a_r(kT) \ , \tag{7}$$

where a_r denotes the acceleration of the refuge. The proposed combined model augments the existing fish state space by introducing two new variables. This expansion results in the fish's state space, encompassing its position and velocity attributes, transitioning into a four-dimensional domain. To align with the prospective state estimation framework, the state space takes the form of

$$\boldsymbol{z} = \begin{bmatrix} \boldsymbol{x} \\ \boldsymbol{q} \end{bmatrix} \text{ where } \boldsymbol{q} = \begin{bmatrix} p_r - p_x \\ v_r - v_x \end{bmatrix}. \tag{8}$$

By combining the models given in Eq. (6) and Eq. (7), the new state space transition equation can be expressed as

$$\boldsymbol{z}\left((k+1)T\right) = \underbrace{\begin{bmatrix} A_f & \mathbf{0} \\ A_r - A_f & A_r \end{bmatrix}}_{\mathrm{A}} \boldsymbol{z}\left(kT\right) + \underbrace{\begin{bmatrix} B_f & \mathbf{0} \\ -B_f & B_r \end{bmatrix}}_{\mathrm{B}} \begin{bmatrix} u(kT) + \omega(kT) \\ a_r(kT) \end{bmatrix}. \tag{9}$$

It is important to note that the fish's perception of its refuge is modeled with a constant velocity approach, and the inclusion of $a_r(kT)$ in this equation accounts for the uncertainty inherent in the fish's perception. So, it is also modeled as a zero-mean Gaussian distribution with a standard deviation of σ_a in the state estimation framework. Moreover, we assume that the fish produces two motion inputs, $u = u_c + u_a$, one for achieving the tracking control, u_c, and one for active sensing generation, u_a. The schematic representation of this model is depicted in Fig. 2.

4.3.2 Controller Design and Implementation

As previously presented, locomotion behavior relies on two distinct objectives: refuge tracking and enhancement of sensory salience. In our model, we assume that the neural controller generates two control inputs, a tracking controller and an active sensing movement generator, to achieve these objectives. Our primary objective is to find models for these controllers that can explain experimental data. To facilitate this pursuit, we initially undertake the system identification of the task-level controller governing fish behavior within an illuminated environment. This choice is motivated by the observation of a diminished incidence of active sensing movements in such conditions. In that

respect, we assume that the active sensing movement generator is either non-active or active sensing movement outputs are quite small compared to the tracking controller outputs, thereby allowing us to identify parameters that are not associated with the active sensing.

To this end, we first concentrate on the whole input-output dynamics and a second-order model, expressed as:

$$G(s) = (Aw_n^2)/(s^2 + 2\zeta w_n s + w_n^2). \tag{10}$$

This model, initially proposed by Cowan & Fortune [34], can effectively capture the input-output dynamics displayed by the fish. Consistent with Uyanik et al. [35], we undertake a parametric system identification process to reveal the underlying closed-loop eigenvalues of the dynamics for $N = 3$ fish. In these experiments, tests were conducted under a well-lit environment, specifically at 300 lux. The refuge was subjected to a constant-frequency sinusoidal input, with frequencies set at 0.10 Hz, 0.15 Hz, and 0.25 Hz. For each frequency, a series of 10 experiments was performed, resulting in a total of 30 distinct trials. To facilitate the system identification process, we employed MATLAB's "greyest" function. This method was applied using all 30 experiments to determine the parameters specified in equation Eq. (10) for each fish. The outcomes of this identification process are tabulated in Table 3.

Building on this, we formulate a state feedback mechanism using the pole placement technique for the tracking controller. This approach is combined with the earlier mentioned plant model presented in equation Eq. (1), with the objective of aligning the closed-loop eigenvalues to the positions acquired from the parametric system identification process.

Table 3 Estimated parameters of second order input-output model, Eq. (10) for each fish and corresponding eigen values

	Fish 1	Fish 2	Fish 3
A	1.01	0.98	0.88
ζ	0.58	0.80	1.15
w_n	9.11	7.73	9.37
$\lambda_{1,2}$[1]	$0.77 + 0.24i$	$0.79 + 0.15i$	0.81
	$0.77 - 0.24i$	$0.79 - 0.15i$	0.52

[1]Closed-loop eigen values of $G(s)$ after discretization under zero-order hold operation with sampling time $T = 0.04$ s for given parameters.

4.3.3 State Estimation Framework

Fish exhibit complex behaviors that demand a robust framework for state (body & target) estimation. This need becomes particularly important when considering the dual objectives of tracking refuge and enhancing sensory salience.

The equation Eq. (7) captures the discrete state transition dynamics of augmented system dynamics, whereas equation Eq. (3) details the continuous measurement model. In parallel with out mathematical and data analysis framework, we also discretize this measurement model as

$$y(kT) = ap_q(kT)v_q(kT) + bv_q(kT) + \rho(kT). \tag{11}$$

Here, we denote the measurement noise by ρ, which follows a zero-mean Gaussian distribution with a standard deviation of σ_ρ. Although the system dynamics are linear, the measurement model is nonlinear. In order to address this nonlinearity in the state estimation approach, we adopt the Extended Kalman Filter (EKF).

4.4 System Identification of Active Sensing

As discussed previously, we identified several parameters non-associated with the active sensing generator or state estimator based on experimental data collected under well-lit conditions. Here, we aim to identify parameters associated explicitly with the estimation and active sensing operators. We conducted this system identification process by developing an optimization framework that utilizes Matlab's particle swarm optimization algorithm. The optimization's objective function was constructed around the MMD metric, enabling a comparative analysis between the frequency domain representations of the simulated fish data—generated from stochastic Monte-Carslo simulations (N =1000)—and the actual fish observational data. These observations were specific to individual fish subjected to selected stimulus frequencies, namely 0.10 Hz, 0.15 Hz, or 0.25 Hz. To ensure the stability of the closed-loop system, a penalty function method was integrated into the objective function, a common approach in system identification. The process involved transforming the time domain data of both the simulated and observed fish into the frequency domain using the Discrete Fourier Transform, followed by the evaluation of MMD between these transformed datasets. The optimization algorithm's goal was to minimize the MMD, thereby aligning the simulated data with the empirical observations as closely as possible. Further details on the implementation of MMD are provided in Section 4.6.2.

In the Monte-Carlo simulations, we set the task-level controller parameters for the given fish based on the findings presented in Table 3. The initial conditions for the simulated fish—position, and velocity—were uniformly distributed around the refuge's initial state to mirror the natural starting conditions. To eliminate the influence of transient dynamics on the frequency domain data, our analysis concentrated on the final 40 seconds of each 60-second simulation run, a mandatory process in frequency domain system identification and analysis.

The parameters subject to optimization are the scene parameters as described in Eq. (3) and the standard deviations of the noise parameters, specifically σ_ρ and σ_a. In our simulations, We kept the standard deviation of

process noise constant at $\sigma_w = 0.01$. In addition to these, we also adjusted parameters related to the active sensing generation block, which vary based on the specific model in use. For the alternating model and the model proposed by Biswas et al. (2023) [25], we considered three parameters: the threshold pair and the Gaussian input standard deviation. The open-loop model utilized a single parameter, the Gaussian input standard deviation, while the predictive uncertainty model incorporated the γ_i's in Eq. (4).

4.5 Neural network implementation of active sensing generation

The architecture of the Artificial Neural Networks (ANNs) employed in our investigation is depicted in Fig. 5A. The feedforward neural network comprises three primary layers: the input layer with six neurons, a single hidden layer containing twenty neurons, and an output layer with a single neuron. The input layer receives the system's state and the variances of the relative position and velocity, while the output is designed to generate the active sensing input. The optimal neuron count for the hidden layer was determined through an iterative trial-and-error methodology.

For the development and execution of the ANNs, we utilized MATLAB's Neural Network Toolbox. The dataset for our study encompassed 10 simulations, each conducted under identical settings at a fixed frequency. This dataset was randomly partitioned into two subsets using MATLAB's dividerand function: 85% was allocated for training purposes, and the remaining 15% constituted the testing set. The training of the ANN was facilitated by a back-propagation algorithm, specifically the Levenberg-Marquardt method, with the Mean Squared Error as the performance metric. The training regimen was terminated upon the fulfillment of any of the following criteria: (1) the attainment of the maximum iteration count of 1000, (2) the achievement of a satisfactory performance level, (3) the reduction of the estimation error to below the predefined threshold, or (4) the escalation of the Levenberg-Marquardt adjustment parameter beyond the value of 10^{10}.

4.6 Computational Methods for Statistical Analysis

4.6.1 Bootstrap Confidence Interval Analysis

To evaluate the consistency of the frequency magnitudes obtained from the Discrete Fourier Transform of positional data, we employed a bootstrap resampling method. This approach involved creating 10,000 bootstrap samples from the original magnitude data, each sample being drawn with replacement to maintain the original sample size. For each resampled dataset, we computed the mean magnitude across all frequencies to form a distribution of mean values. The 95% confidence intervals for the mean magnitudes were then established using the $2.5th$ and $97.5th$ percentiles of this bootstrap distribution. This technique allowed us to infer the variability and confidence of the periodic components detected in the positional data without relying on parametric

assumptions, which is particularly advantageous for non-Gaussian or small sample size data.

4.6.2 Maximum Mean Discrepancy (MMD) Evaluation

Maximum mean discrepancy [40] serves as a non-parametric statistical metric that measures the disparity between two probability distributions. It is a common method used in machine learning literature, particularly in the context of kernel methods and in scenarios such as domain adaptation, transfer learning, and two-sample testing. Here, this metric offers a reliable way to contrast simulated fish data with experimental observations. Its ability to handle complex distributions without specific form assumptions sets it apart as a valuable tool in assessing model accuracy and fit.

The Maximum Mean Discrepancy (MMD) is a measure of the distance between two probability distributions, $\mathbb{P}$ and $\mathbb{Q}$, based on the mean embeddings in a Reproducing Kernel Hilbert Space (RKHS). The RKHS is a space of functions endowed with a kernel function k, which is symmetric and positive definite. This kernel function implicitly maps data to a high-dimensional feature space and measures the similarity between data points. The kernel embedding of a distribution $\mathbb{P}$ is a function $\mu_{\mathbb{P}}$ in the RKHS defined by the expectation of the feature map associated with k:

$$\mu_{\mathbb{P}} = \mathbb{E}_{X\sim\mathbb{P}}[k(\cdot, X)]$$

This embedding captures all the moments of the distribution, assuming the kernel k is characteristic. For two distributions $\mathbb{P}$ and $\mathbb{Q}$, their MMD is defined as the RKHS norm of the difference between their embeddings:

$$\mathrm{MMD}(\mathbb{P}, \mathbb{Q}) = \|\mu_{\mathbb{P}} - \mu_{\mathbb{Q}}\|_{\mathcal{H}}$$

In practice, we don't have access to the distributions directly but rather samples from them. Given samples $\{X_i\}_{i=1}^n$ from $\mathbb{P}$ and $\{Y_i\}_{i=1}^m$ from $\mathbb{Q}$, the empirical estimate of the squared MMD is:

$$\begin{aligned}\mathrm{MMD}_u^2(\mathbb{P}, \mathbb{Q}) =& \frac{1}{n(n-1)} \sum_{\substack{i,j \\ i\neq j}} k\left(X_i, X_j\right) + \frac{1}{m(m-1)} \sum_{\substack{i,j \\ i\neq j}} k\left(Y_i, Y_j\right) \\ &- \frac{2}{nm} \sum_{i,j} k\left(x_i, y_j\right)\end{aligned}$$

This expression is computationally feasible and does not require explicit computation of the feature maps. It involves only the kernel function evaluations, which are often much simpler to compute. For the results presented in the study, we used this formula and the Gaussian kernel $k : x, y \to k(x, y) = \frac{1}{\sqrt{2\pi}\sigma} \exp\left(-\frac{\|x-y\|_2^2}{2\sigma^2}\right)$. We set the kernel bandwidth as $\sigma = 1$. Note that since

this is an unbiased empirical estimation of MMD, it can take negative values if the true MMD value is close to zero. Those negative values are replaced by zeros while presenting the results.

4.6.3 Permutation-Based p-Value Calculation for Two-Sample Test

To determine the statistical significance of the MMD between two samples, we employed a permutation test. This non-parametric approach involves combining the samples and randomly shuffling the pooled observations to generate new sample pairs. For each of the $\mathcal{B}$ permutations, the MMD statistic is recalculated, creating a null distribution of MMD values under the hypothesis that both samples originate from the same distribution. The p-value is then estimated as the proportion of permuted MMD statistics that exceed the observed MMD, with a low p-value indicating a significant difference between the distributions of the two samples. In our study, we set $\mathcal{B}$ to 10,000 permutations to ensure an accurate estimation of the p-value. This approach is particularly advantageous in biological data analysis, where the underlying distributions may not conform to standard parametric assumptions, thus necessitating a flexible and assumption-free test.

4.6.4 Cross-Validation for Model Performance Assessment

To evaluate the predictive ability of our model and illustrate that it does not suffer from overfitting in the parameter estimation step, we implemented a cross-validation strategy. Cross-validation is a robust statistical method used to assess the generalizability of a model to an independent dataset. Specifically, we employed a 3-fold cross-validation approach for the predictive uncertainty model.

The dataset was partitioned into three distinct folds, ensuring that each fold contained a balanced representation of data across all stimulus frequencies. This stratification is crucial to maintain the integrity of the cross-validation process, as it prevents the model from being tested on unrepresentative subsets of data.

For each cross-validation fold, the model was trained on two-thirds of the data (the training set) and tested on the remaining one-third (the test set). The training phase involved adjusting the model parameters to minimize the discrepancy between the model outputs and the observed data as in Section 4.4. The test phase then evaluated the model's performance on the test set, which was not exposed to the model during the training phase.

The model's performance was quantified using the MMD metric, comparing the distribution of the model's predictions to the actual fish data. A p-value was computed to assess the statistical significance of the discrepancy between these distributions, as described in the previous section. A p-value greater than 0.05 indicates that the difference is not statistically significant, suggesting that the model predictions are consistent with the actual data.

References

[1] Nelson, M., MacIver, M.: Sensory acquisition in active sensing systems. Journal of comparative physiology. A, Neuroethology, sensory, neural, and behavioral physiology **192**(6), 573–586 (2006). https://doi.org/10.1007/s00359-006-0099-4

[2] Stamper, S.A., Madhav, M.S., Cowan, N.J., Fortune, E.S.: Using control theory to characterize active sensing in weakly electric fishes. Electroreception: Fundamental Insights from Comparative Approaches, 227–249 (2019)

[3] Dürr, V., Krause, A.F.: In: Jaeger, D., Jung, R. (eds.) Tactile Sensing in Insects, pp. 1–5. Springer, New York, NY (2013). https://doi.org/10.1007/978-1-4614-7320-6_641-1. https://doi.org/10.1007/978-1-4614-7320-6_641-1

[4] Fuchs, A.F.: Saccadic and smooth pursuit eye movements in the monkey. The Journal of Physiology **191**(3), 609–631 (1967) https://arxiv.org/abs/https://physoc.onlinelibrary.wiley.com/doi/pdf/10.1113/jphysiol.1967.sp008271. https://doi.org/10.1113/jphysiol.1967.sp008271

[5] Bush, N.E., Solla, S.A., Hartmann, M.J.: Whisking mechanics and active sensing. Current Opinion in Neurobiology **40**, 178–188 (2016). https://doi.org/10.1016/j.conb.2016.08.001. Systems neuroscience

[6] Schroeder, C.E., Wilson, D.A., Radman, T., Scharfman, H., Lakatos, P.: Dynamics of active sensing and perceptual selection. Current Opinion in Neurobiology **20**(2), 172–176 (2010). https://doi.org/10.1016/j.conb.2010.02.010. Cognitive neuroscience

[7] Biswas, D., Arend, L.A., Stamper, S.A., Vágvölgyi, B.P., Fortune, E.S., Cowan, N.J.: Closed-loop control of active sensing movements regulates sensory slip. Current Biology **28**(24), 4029–4036 (2018)

[8] König, P., Luksch, H.: Active sensing-closing multiple loops. Zeitschrift für Naturforschung C **53**(7-8), 542–549 (1998)

[9] Schuster, S.: Active sensing: Matching motor and sensory space. Current Biology **18**(4), 176–178 (2008). https://doi.org/10.1016/j.cub.2007.12.005

[10] Jones, T.K., Allen, K.M., Moss, C.F.: Communication with self, friends and foes in active-sensing animals. Journal of Experimental Biology **224**(22), 242637 (2021) https://arxiv.org/abs/https://journals.biologists.com/jeb/article-pdf/224/22/jeb242637/2118976/jeb242637.pdf. https://doi.org/10.1242/jeb.242637

[11] Schabacker, T., Lindecke, O., Rizzi, S., Marggraf, L., Pētersons, G., Voigt, C., Snijders, L.: In situ novel environment assay reveals acoustic exploration as a repeatable behavioral response in migratory bats. Scientific Reports **11**(1) (2021). https://doi.org/10.1038/s41598-021-87588-y. Publisher Copyright: © 2021, The Author(s). Copyright: Copyright 2021 Elsevier B.V., All rights reserved.

[12] Jun, J.J., Longtin, A., Maler, L.: Active sensing associated with spatial learning reveals memory-based attention in an electric fish. Journal of Neurophysiology **115**(5), 2577–2592 (2016)

[13] Yeo, S.-H., Franklin, D.W., Wolpert, D.M.: When optimal feedback control is not enough: Feedforward strategies are required for optimal control with active sensing. PLOS Computational Biology **12**(12), 1–22 (2016). https://doi.org/10.1371/journal.pcbi.1005190

[14] Yoon, J., Zame, W.R., van der Schaar, M.: Deep sensing: Active sensing using multi-directional recurrent neural networks. In: International Conference on Learning Representations (2018). https://openreview.net/forum?id=r1SnX5xCb

[15] Zweifel, N.O., Hartmann, M.J.Z.: Defining "active sensing" through an analysis of sensing energetics: homeoactive and alloactive sensing. Journal of Neurophysiology **124**(1), 40–48 (2020) https://arxiv.org/abs/https://doi.org/10.1152/jn.00608.2019. https://doi.org/10.1152/jn.00608.2019. PMID: 32432502

[16] Deutsch, D., Pietr, M., Knutsen, P.M., Ahissar, E., Schneidman, E.: Fast feedback in active sensing: touch-induced changes to whisker-object interaction (2012)

[17] Okada, J., Toh, Y.: Active tactile sensing for localization of objects by the cockroach antenna. Journal of comparative physiology. A, Neuroethology, sensory, neural, and behavioral physiology **192**(7), 715–726 (2006). https://doi.org/10.1007/s00359-006-0106-9

[18] Chen, C., Murphey, T.D., MacIver, M.A.: Tuning movement for sensing in an uncertain world. eLife **9**, 52371 (2020). https://doi.org/10.7554/eLife.52371

[19] Nakata, K.: Attention focusing in a sit-and-wait forager: a spider controls its prey-detection ability in different web sectors by adjusting thread tension. Proceedings of the Royal Society B: Biological Sciences **277**(1678), 29–33 (2010)

[20] Blamires, S.J., Chao, Y.-C., Liao, C.-P., Tso, I.-M.: Multiple prey cues induce foraging flexibility in a trap-building predator. Animal Behaviour

81(5), 955–961 (2011)

[21] Uyanik, I., Stamper, S.A., Cowan, N.J., Fortune, E.S.: Sensory cues modulate smooth pursuit and active sensing movements. Frontiers in Behavioral Neuroscience **13** (2019). https://doi.org/10.3389/fnbeh.2019.00059

[22] Crimaldi, J., Lei, H., Schaefer, A., Schmuker, M., Smith, B., True, A., Verhagen, J., Victor, J.: Active sensing in a dynamic olfactory world. Journal of Computational Neuroscience **50** (2021). https://doi.org/10.1007/s10827-021-00798-1

[23] Claverie, N., Buvat, P., Casas, J.: Active Sensing in Bees Through Antennal Movements Is Independent of Odor Molecule. Integrative and Comparative Biology **63**(2), 315–331 (2023) https://arxiv.org/abs/https://academic.oup.com/icb/article-pdf/63/2/315/51233028/icad010.pdf. https://doi.org/10.1093/icb/icad010

[24] Hofmann, V., Sanguinetti-Scheck, J.I., Künzel, S., Geurten, B., Gómez-Sena, L., Engelmann, J., Krahe, R., Fortune, E.: Sensory flow shaped by active sensing: sensorimotor strategies in electric fish. Journal of Experimental Biology **216**(13), 2487–2500 (2013) https://arxiv.org/abs/https://journals.biologists.com/jeb/article-pdf/216/13/2487/1284617/2487.pdf. https://doi.org/10.1242/jeb.082420

[25] Biswas, D., Lamperski, A., Yang, Y., Hoffman, K., Guckenheimer, J., Fortune, E., Cowan, N.: Mode switching in organisms for solving explore-versus-exploit problems. Nature Machine Intelligence (2023). https://doi.org/10.1038/s42256-023-00745-y. https://www.nature.com/articles/s42256-023-00745-y

[26] Manjarrez, E., Rojas-Piloni, G., Méndez, I., Flores, A.: Stochastic resonance within the somatosensory system: Effects of noise on evoked field potentials elicited by tactile stimuli. Journal of Neuroscience **23**(6), 1997–2001 (2003) https://arxiv.org/abs/https://www.jneurosci.org/content/23/6/1997.full.pdf. https://doi.org/10.1523/JNEUROSCI.23-06-01997.2003

[27] Moss, F., Ward, L.M., Sannita, W.G.: Stochastic resonance and sensory information processing: a tutorial and review of application. Clinical neurophysiology **115**(2), 267–281 (2004)

[28] Ward, L., Neiman, A., Moss, F.: Stochastic resonance in psychophysics and in animal behavior. Biological cybernetics **87**, 91–101 (2002). https://doi.org/10.1007/s00422-002-0328-z

[29] Yang, Y.: A comparison of system identification techniques for refuge

tracking behavior in eigenmannia virescens. PhD thesis, Johns Hopkins University (2020)

[30] Yared, D.G.: Learning of novel dynamics in eigenmannia virescens refuge tracking task. PhD thesis, Johns Hopkins University (2020)

[31] Roth, E., Zhuang, K., Stamper, S.A., Fortune, E.S., Cowan, N.J.: Stimulus predictability mediates a switch in locomotor smooth pursuit performance for Eigenmannia virescens. Journal of Experimental Biology **214**(7), 1170–1180 (2011) https://arxiv.org/abs/https://journals.biologists.com/jeb/article-pdf/214/7/1170/1278821/1170.pdf. https://doi.org/10.1242/jeb.048124

[32] Sutton, E.E., Demir, A., Stamper, S.A., Fortune, E.S., Cowan, N.J.: Dynamic modulation of visual and electrosensory gains for locomotor control. Journal of The Royal Society Interface **13**(118), 20160057 (2016)

[33] von der Emde, G.: Active electrolocation of objects in weakly electric fish. Journal of Experimental Biology **202**(10), 1205–1215 (1999) https://arxiv.org/abs/https://journals.biologists.com/jeb/article-pdf/202/10/1205/3107677/jexbio_202_10_1205.pdf. https://doi.org/10.1242/jeb.202.10.1205

[34] Cowan, N.J., Fortune, E.S.: The critical role of locomotion mechanics in decoding sensory systems. Journal of Neuroscience **27**(5), 1123–1128 (2007)

[35] Uyanik, I., Sefati, S., Stamper, S.A., Cho, K.-A., Ankarali, M.M., Fortune, E.S., Cowan, N.J.: Variability in locomotor dynamics reveals the critical role of feedback in task control. Elife **9**, 51219 (2020)

[36] Stamper, S.A., Roth, E., Cowan, N.J., Fortune, E.S.: Active sensing via movement shapes spatiotemporal patterns of sensory feedback. Journal of Experimental Biology **215**(9), 1567–1574 (2012)

[37] Sefati, S., Neveln, I.D., Roth, E., Mitchell, T.R., Snyder, J.B., MacIver, M.A., Fortune, E.S., Cowan, N.J.: Mutually opposing forces during locomotion can eliminate the tradeoff between maneuverability and stability. Proceedings of the national academy of sciences **110**(47), 18798–18803 (2013)

[38] Kunapareddy, A., Cowan, N.J.: Recovering observability via active sensing. In: 2018 Annual American Control Conference (ACC), pp. 2821–2826 (2018). IEEE

[39] Comertler, M.S., Uyanik, I.: Salience of multisensory feedback regulates behavioral variability. Bioinspiration & Biomimetics **17**(1), 016006 (2021)

[40] Gretton, A., Borgwardt, K.M., Rasch, M.J., Schölkopf, B., Smola, A.: A kernel two-sample test. The Journal of Machine Learning Research **13**(1), 723–773 (2012)

[41] Feldman, A.G.: Active sensing without efference copy: referent control of perception. Journal of neurophysiology **116**(3), 960–976 (2016)

[42] Yang, S.C.-H., Lengyel, M., Wolpert, D.M.: Active sensing in the categorization of visual patterns. eLife **5**, 12215 (2016). https://doi.org/10.7554/eLife.12215

[43] Wachowiak, M.: All in a sniff: olfaction as a model for active sensing. Neuron **71**(6), 962–973 (2011)

[44] Ryan, A., Hedrick, J.K.: Particle filter based information-theoretic active sensing. Robotics and Autonomous Systems **58**(5), 574–584 (2010)

[45] Cognetti, M., Salaris, P., Robuffo Giordano, P.: Optimal active sensing with process and measurement noise. In: 2018 IEEE International Conference on Robotics and Automation (ICRA), pp. 2118–2125 (2018). https://doi.org/10.1109/ICRA.2018.8460476

[46] Solopchuk, O., Zénon, A.: Active sensing with artificial neural networks. Neural Networks **143**, 751–758 (2021). https://doi.org/10.1016/j.neunet.2021.08.007

[47] Yeo, S.-H., Franklin, D.W., Wolpert, D.M.: When optimal feedback control is not enough: Feedforward strategies are required for optimal control with active sensing. PLoS computational biology **12**(12), 1005190 (2016)

[48] Leszczynski, M., Schroeder, C.E.: The role of neuronal oscillations in visual active sensing. Frontiers in integrative neuroscience **13**, 32 (2019)

[49] Mitchinson, B., Prescott, T.J.: Whisker movements reveal spatial attention: a unified computational model of active sensing control in the rat. PLoS computational biology **9**(9), 1003236 (2013)

[50] Bar-Shalom, Y., Birmiwal, K.: Variable dimension filter for maneuvering target tracking. IEEE transactions on Aerospace and Electronic Systems (5), 621–629 (1982)

[51] Pellegrini, S., Ess, A., Schindler, K., Van Gool, L.: You'll never walk alone: Modeling social behavior for multi-target tracking. In: 2009 IEEE 12th International Conference on Computer Vision, pp. 261–268 (2009). IEEE

[52] Mahmoudi, N., Ahadi, S.M., Rahmati, M.: Multi-target tracking using cnn-based features: Cnnmtt. Multimedia Tools and Applications **78**,

7077–7096 (2019)